
Neural Flow Diffusion Models: Learnable Forward Process for Improved Diffusion Modelling

Grigory Bartosh¹ Dmitry Vetrov² Christian A. Naesseth¹

Abstract

Conventional diffusion models typically relies on a fixed forward process, which implicitly defines complex marginal distributions over latent variables. This can often complicate the reverse process' task in learning generative trajectories, and results in costly inference for diffusion models. To address these limitations, we introduce Neural Flow Diffusion Models (NFDM), a novel framework that enhances diffusion models by supporting a broader range of forward processes beyond the fixed linear Gaussian. We also propose a novel parameterization technique for learning the forward process. Our framework provides an end-to-end, simulation-free optimization objective, effectively minimizing a variational upper bound on the negative log-likelihood. Experimental results demonstrate NFDM's strong performance, evidenced by state-of-the-art likelihood estimation. Furthermore, we investigate NFDM's capacity for learning generative dynamics with specific characteristics, such as deterministic straight lines trajectories. This exploration underscores NFDM's versatility and its potential for a wide range of applications.

1. Introduction

Generative models are a versatile class of probabilistic machine learning models, which finds applications across diverse fields such as art, music, medicine, and physics (Tomczak, 2022; Creswell et al., 2018; Papamakarios et al., 2021; Yang et al., 2022). Generative models excel in constructing probability distributions that accurately represent datasets, enabling them to produce new samples akin to the original data. Such capabilities make them ideal for tasks like enhancing training data through the generation of syn-

thetic datasets (data augmentation) and uncovering hidden patterns and structures in an unsupervised learning setting.

Diffusion models (Sohl-Dickstein et al., 2015; Ho et al., 2020) are a class of generative models are constructed by two key processes: the forward process and the reverse process. The forward process gradually corrupts the data distribution, transforming it from its original form to a noised state. The reverse process learns to invert corruptions of the forward process and restore the data distribution. This way, it learns to generate data from pure noise. Diffusion models have demonstrated remarkable results in various domains (Ho et al., 2022; Saharia et al., 2022; Tan et al., 2024; Watson et al., 2023; Trippe et al., 2023). Nevertheless, most existing diffusion models fix the forward process to be pre-defined Gaussian, which makes it unable to adapt to the task at hand or simplify the target for the reverse process. At the same time there are many works that demonstrate how modifications of the forward process improve performance in terms of generation quality (Nichol & Dhariwal, 2021; Vahdat et al., 2021; Daras et al., 2022), likelihood estimation (Kingma et al., 2021; Nielsen et al., 2023; Bartosh et al., 2023) or sampling speed (Lee et al., 2023; Pooladian et al., 2023; Tong et al., 2023).

In this paper, we present Neural Flow Diffusion Models (NFDM), a framework that allows for the pre-specification and learning of latent variable distributions defined by the forward process. Unlike conventional diffusion models (Ho et al., 2020), which rely on a conditional Gaussian forward process, NFDM may accommodate any continuous (and learnable) distribution that can be expressed as an invertible mapping applied to noise. We also derive, and leverage, an end-to-end simulation-free optimization procedure, that minimizes a variational upper bound on the negative log-likelihood (NLL).

We also propose an efficient neural network-based parameterization for the forward process, enabling it to adapt to the reverse process during training and simplify the learning of the data distribution. To demonstrate NFDM's capabilities with a learnable forward process we provide experimental results on CIFAR-10, ImageNet 32 and 64, attaining state-of-the-art NLL results, which is crucial for many applications such as data compression (Ho et al., 2021; Yang &

¹University of Amsterdam ²Constructor University, Bremen. Correspondence to: Grigory Bartosh <g.bartosh@uva.nl>, Dmitry Vetrov <dvetrov@constructor.university>, Christian A. Naesseth <c.a.naesseth@uva.nl>.

Mandt, 2022), anomaly detection (Chen et al., 2018b; Dias et al., 2020) and out-of-distribution detection (Serrà et al., 2019; Xiao et al., 2020).

Leveraging the flexibility of NFDM, we further explore training with constraints on the reverse process to learn generative dynamics with specific properties. As a case study, we discuss a curvature penalty on the deterministic generative trajectories. Our empirical results indicate improved computational efficiency compared to baselines on synthetic datasets as well as MNIST, CIFAR-10, and downsampled ImageNet.

We summarize our contributions as follows:

1. We introduce Neural Flow Diffusion Models (NFDM), improving diffusion modelling through a learnable forward process.
2. We develop an end-to-end optimization procedure that minimizes an upper bound on the negative log-likelihood in a simulation-free manner.
3. We demonstrate state-of-the-art log-likelihood results on CIFAR-10, ImageNet 32 and 64.
4. We show how NFDM can be used in learning generative processes with specific properties, exemplified by dynamics with straight line trajectories, where NFDM leads to significantly faster sampling speeds and enhanced generation quality with fewer sampling steps.

2. Background

Diffusion models are generative latent variable models consisting of two processes: the forward and the reverse (or generative) process. The forward process is a dynamic process that takes a data point $\mathbf{x} \sim q(\mathbf{x})$, $\mathbf{x} \in \mathbb{R}^D$, and perturbs it over time by injecting noise. This generates a trajectory of latent variables $\{\mathbf{z}(t)\}_{t \in [0,1]}$, conditional on the data \mathbf{x} , where $[0, 1]$ is a fixed time horizon and $\mathbf{z}_t = \mathbf{z}(t) \in \mathbb{R}^D$. The (conditional) distribution can be described by an initial distribution $q(\mathbf{z}_0|\mathbf{x})$ and a Stochastic Differential Equation (SDE) with a linear drift term $\tilde{f}^F(\mathbf{z}_t, t) : \mathbb{R}^D \times [0, 1] \mapsto \mathbb{R}^D$, scalar variance $g(t) : [0, 1] \mapsto \mathbb{R}_+$, and a standard Wiener process \mathbf{w} :

$$d\mathbf{z}_t = \tilde{f}^F(\mathbf{z}_t, t)dt + g(t)d\mathbf{w}. \quad (1)$$

Due to the linearity of \tilde{f}^F , we can reconstruct the conditional marginal distribution $q(\mathbf{z}_t|\mathbf{x}) = \mathcal{N}(\mathbf{z}_t; \alpha_t\mathbf{x}, \sigma_t^2 I)$. Typically, the conditional distributions evolve from some low variance distribution $q(\mathbf{z}_0|\mathbf{x}) \approx \delta(\mathbf{z}_0 - \mathbf{x})$ to a unit Gaussian $q(\mathbf{z}_1|\mathbf{x}) \approx \mathcal{N}(\mathbf{z}_1; 0, I)$. This forward process is then reversed by starting from the prior $\mathbf{z}_1 \sim \mathcal{N}(\mathbf{z}_1; 0, I)$,

and following the reverse SDE (Anderson, 1982):

$$d\mathbf{z}_t = \tilde{f}^B(\mathbf{z}_t, t)dt + g(t)d\bar{\mathbf{w}}, \quad \text{where} \quad (2)$$

$$\tilde{f}^B(\mathbf{z}_t, t) = \tilde{f}^F(\mathbf{z}_t, t) - g^2(t)\nabla_{\mathbf{z}_t} \log q_\varphi(\mathbf{z}_t). \quad (3)$$

Here, $\bar{\mathbf{w}}$ denotes a standard Wiener process where time flows backwards. Diffusion models approximate this reverse process by learning $\nabla_{\mathbf{z}_t} \log q(\mathbf{z}_t)$, known as the score function, through a λ_t -weighted score matching loss:

$$\mathbb{E}_{u(t)q(\mathbf{z}_t)} \left[\lambda_t \left\| s_\theta(\mathbf{z}_t, t) - \nabla_{\mathbf{z}_t} \log q_\varphi(\mathbf{z}_t) \right\|_2^2 \right], \quad (4)$$

where $u(t)$ represents a uniform distribution over the interval $[0, 1]$, and $s_\theta : \mathbb{R}^D \times [0, 1] \mapsto \mathbb{R}^D$ is a learnable approximation. This loss can be reformulated as a more tractable denoising score matching loss Vincent (2011):

$$\mathbb{E}_{u(t)q(\mathbf{x}, \mathbf{z}_t)} \left[\lambda_t \left\| s_\theta(\mathbf{z}_t, t) - \nabla_{\mathbf{z}_t} \log q_\varphi(\mathbf{z}_t|\mathbf{x}) \right\|_2^2 \right]. \quad (5)$$

With a learned score function $s_\theta(\mathbf{z}_t, t)$, one can generate a sample from the reverse process by first sampling from the prior $\mathbf{z}_1 \sim \mathcal{N}(\mathbf{z}_1; 0, I)$, and then simulating the reverse SDE:

$$d\mathbf{z}_t = [\tilde{f}^F(\mathbf{z}_t, t) - g^2(t)s_\theta(\mathbf{z}_t, t)]dt + g(t)d\bar{\mathbf{w}}, \quad (6)$$

resulting a sample $\mathbf{z}_0 \sim p_\theta(\mathbf{z}_0) \approx q(\mathbf{z}_0) \approx q(\mathbf{x})$.

Diffusion models possess several important properties. For example, for specific λ_t , the objective (eq. (5)) can be reformulated (Song et al., 2021) as an Evidence Lower Bound (ELBO) on the model’s likelihood. Furthermore, the minimization of denoising score matching (eq. (5)) is a simulation-free procedure. This means that simulating either the forward or reverse processes through its SDE is not necessary for sampling \mathbf{z}_t , nor is it necessary for estimating the gradient of the loss function. Instead, we can directly sample $\mathbf{z}_t \sim q(\mathbf{z}_t|\mathbf{x})$. The simulation-free nature of this approach is a crucial aspect for efficient optimization.

Another notable property is the existence of an Ordinary Differential Equation (ODE) corresponding to the same marginal densities $q(\mathbf{z}_t)$ as the SDE (eq. (1)):

$$d\mathbf{z}_t = f(\mathbf{z}_t, t)dt, \quad \text{where} \quad (7)$$

$$f(\mathbf{z}_t, t) = \tilde{f}^F(\mathbf{z}_t, t) - \frac{g^2(t)}{2} \nabla_{\mathbf{z}_t} \log q_\varphi(\mathbf{z}_t). \quad (8)$$

This implies that we can sample from diffusion models deterministically, allowing the use of off-the-shelf numerical ODE solvers for sampling, which may improve the sampling speed compared to stochastic sampling that requires simulating an SDE. Additionally, deterministic sampling enables us to compute densities by treating the model as a continuous normalizing flow, as detailed in Chen et al. (2018a); Grathwohl et al. (2018).

3. Neural Flow Diffusion Models

Diffusion models can be viewed as a specific type of hierarchical Variational Autoencoders (VAEs) (Kingma & Welling, 2013; Rezende et al., 2014), where the latent variables are inferred through a pre-specified scaling of the data point and injection of Gaussian noise. However, this formulation limits diffusion models in terms of the flexibility of their latent space, and makes learning of the reverse process more challenging. To address this limitation, we propose a generalized form of data and noise transformations that enables the definition and learning of a broad range of distributions in the latent space beyond the conventional Gaussian.

In this section, we introduce Neural Flow Diffusion Models (NFDM) – a framework that generalizes conventional diffusion models. The key idea in NFDM is to define the forward process implicitly via a learnable transformation $F_\varphi(\varepsilon, t, \mathbf{x})$. This lets the user define a broad range of continuous time and data dependent forward process. Importantly, NFDM retains crucial properties of conventional diffusion models, like likelihood-based and simulation-free training. Previous diffusion models emerge as special cases when the data transformation is linear, time-independent, and/or additive Gaussian. The connections between NFDM and existing models are discussed in Section 6.

3.1. Forward process

The forward process defines a target for the reverse process. It describes the distribution of trajectories $\{\mathbf{z}(t)\}_{t \in [0,1]}$ in the latent space that the reverse process tries to match.

We approach the forward process constructively. First, we define a conditional marginal distribution $q_\varphi(\mathbf{z}_t|\mathbf{x})$ for $t \in [0, 1]$. Then, we introduce the corresponding conditional ODE that together with the initial distribution $q_\varphi(\mathbf{z}_0|\mathbf{x})$ matches the conditional marginal distribution $q_\varphi(\mathbf{z}_t|\mathbf{x})$. Finally, we define a conditional SDE that implicitly defines distribution over trajectories $\{\mathbf{z}(t)\}_{t \in [0,1]}$, with the same marginal distributions $q_\varphi(\mathbf{z}_t|\mathbf{x})$.

Forward Marginal Distribution. We characterize the marginal distribution $q_\varphi(\mathbf{z}_t|\mathbf{x})$ of the forward process through a function of injected noise ε , time t , and the data \mathbf{x} :

$$\mathbf{z}_t = F_\varphi(\varepsilon, t, \mathbf{x}), \quad (9)$$

where $F_\varphi : \mathbb{R}^D \times [0, 1] \times \mathbb{R}^D \mapsto \mathbb{R}^D$ and $\varepsilon \sim q(\varepsilon) = \mathcal{N}(\varepsilon; 0, I)$. This function transforms a sample from a distribution $q(\varepsilon)$ into \mathbf{z}_t , conditional on the data point \mathbf{x} and time step t , implicitly defining the conditional distribution of latent variables $q_\varphi(\mathbf{z}_t|\mathbf{x})$. Additionally, eq. (9) facilitates direct and efficient sampling from $q_\varphi(\mathbf{z}_t|\mathbf{x})$ through F_φ .

Conditional ODE. Assuming that F_φ is differentiable with respect to ε and t and invertible with respect to ε , fixing

specific values of \mathbf{x} and ε and varying t from 0 to 1 results in a smooth trajectory from \mathbf{z}_0 to \mathbf{z}_1 . Differentiating these trajectories over time yields a velocity field corresponding to the conditional distribution $q_\varphi(\mathbf{z}_t|\mathbf{x})$, thereby defining a conditional ODE:

$$d\mathbf{z}_t = f_\varphi(\mathbf{z}_t, t, \mathbf{x})dt, \quad \text{where} \quad (10)$$

$$f_\varphi(\mathbf{z}_t, t, \mathbf{x}) = \left. \frac{\partial F_\varphi(\varepsilon, t, \mathbf{x})}{\partial t} \right|_{\varepsilon=F_\varphi^{-1}(\mathbf{z}_t, t, \mathbf{x})}. \quad (11)$$

Therefore, if we sample $\mathbf{z}_0 \sim q_\varphi(\mathbf{z}_0|\mathbf{x})$ and solve the ODE in eq. (10) until time t , we have a sample $\mathbf{z}_t \sim q_\varphi(\mathbf{z}_t|\mathbf{x})$.

The time derivative of F_φ may be calculated using automatic differentiation tools like PyTorch (Paszke et al., 2017) or JAX (Bradbury et al., 2018). Specifically, we can compute a Jacobian Vector Product (JVP) with a unit one-dimensional vector. Unlike standard backpropagation, which corresponds to a Vector Jacobian Product (VJP), JVP does not necessitate $\mathcal{O}(D)$ backpropagation passes, enhancing scalability.

Conditional SDE. The function F_φ and the distribution of the noise $q(\varepsilon)$ together defines $q_\varphi(\mathbf{z}_0|\mathbf{x})$. To completely define the distribution of trajectories $\{\mathbf{z}(t)\}_{t \in [0,1]}$, we introduce a conditional SDE that starts from sample \mathbf{z}_0 and runs forward in time.

With access to both the ODE and score function $\nabla_{\mathbf{z}_t} \log q_\varphi(\mathbf{z}_t|\mathbf{x})$, the SDE (Song et al., 2020b) corresponding to the distribution $q_\varphi(\mathbf{z}_t|\mathbf{x})$, is:

$$d\mathbf{z}_t = \tilde{f}_\varphi^F(\mathbf{z}_t, t, \mathbf{x})dt + g_\varphi(t)d\mathbf{w}, \quad \text{where} \quad (12)$$

$$\tilde{f}_\varphi^F(\mathbf{z}_t, t, \mathbf{x}) = f_\varphi(\mathbf{z}_t, t, \mathbf{x}) + \frac{g_\varphi^2(t)}{2} \nabla_{\mathbf{z}_t} \log q_\varphi(\mathbf{z}_t|\mathbf{x}).$$

Here, $g_\varphi : [0, 1] \mapsto \mathbb{R}_+$ is a scalar function, and \mathbf{w} represents a standard Wiener process. It is important to note, that g_φ only influences the distribution of trajectories $\{\mathbf{z}(t)\}_{t \in [0,1]}$, not the marginal distributions. The Conditional SDE in eq. (12) has the same conditional marginal distribution, $q_\varphi(\mathbf{z}_t|\mathbf{x})$, for any g_φ .

The score function of $q_\varphi(\mathbf{z}_t|\mathbf{x})$ is:

$$\nabla_{\mathbf{z}_t} \log q_\varphi(\mathbf{z}_t|\mathbf{x}) = \nabla_{\mathbf{z}_t} [\log q(\varepsilon) + \log |J_F^{-1}|] \quad (13)$$

$$\varepsilon = F_\varphi^{-1}(\mathbf{z}_t, t, \mathbf{x}) \quad \text{and} \quad J_F^{-1} = \frac{\partial F_\varphi^{-1}(\mathbf{z}_t, t, \mathbf{x})}{\partial \mathbf{z}_t}. \quad (14)$$

While the log-determinant of the Jacobian matrix J_F^{-1} is not generally available in explicit form, it can be analytically evaluated for certain transformations or specific architectures of the function F_φ , like RealNVP style architectures (Dinh et al., 2016; Kingma & Dhariwal, 2018). The parameterization of F_φ is further discussed in Section 3.5.

Given access to the log probability $\log q(\varepsilon)$ and the log-determinant of J_F^{-1} , automatic differentiation tools enable the calculation of gradients and the score function. Unlike the time derivative, regular backpropagation can be utilized here, ensuring computationally efficient score function evaluation.

3.2. Reverse process

To define the reverse (generative) process, we specify a reverse SDE that starts from $\mathbf{z}_1 \sim p(\mathbf{z}_1)$ and runs backwards in time. To do so we first introduce a conditional reverse SDE that reverses the conditional forward SDE (eq. (12)). Following (Anderson, 1982), we define:

$$d\mathbf{z}_t = \tilde{f}_\varphi^B(\mathbf{z}_t, t, \mathbf{x})dt + g_\varphi(t)d\mathbf{w}, \quad \text{where} \quad (15)$$

$$\tilde{f}_\varphi^B(\mathbf{z}_t, t, \mathbf{x}) = f_\varphi(\mathbf{z}_t, t, \mathbf{x}) - \frac{g_\varphi^2(t)}{2} \nabla_{\mathbf{z}_t} \log q_\varphi(\mathbf{z}_t | \mathbf{x}).$$

Secondly, we reference the reverse SDE (see eq. (15)) and incorporating the prediction of \mathbf{x} :

$$d\mathbf{z}_t = \hat{f}_{\theta, \varphi}(\mathbf{z}_t, t)dt + g_\varphi(t)d\bar{\mathbf{w}}, \quad \text{where} \quad (16)$$

$$\hat{f}_{\theta, \varphi}(\mathbf{z}_t, t) = \tilde{f}_\varphi^B(\mathbf{z}_t, t, \hat{\mathbf{x}}_\theta(\mathbf{z}_t, t)), \quad (17)$$

and $\hat{\mathbf{x}}_\theta : \mathbb{R}^D \times [0, 1] \mapsto \mathbb{R}^D$ is a function that predicts the data point \mathbf{x} . This SDE defines the dynamics of the generative trajectories $\{\mathbf{z}(t)\}_{t \in [0, 1]}$.

However, to fully specify the reverse process, it is necessary to define a prior distribution $p(\mathbf{z}_1)$ and a reconstruction distribution $p(\mathbf{x} | \mathbf{z}_0)$. In all of our experiments, we set the prior $p(\mathbf{z}_1)$ to be a unit Gaussian distribution $\mathcal{N}(\mathbf{z}_1; 0, I)$ and let $p(\mathbf{x} | \mathbf{z}_0)$ be a Gaussian distribution with a small variance $\mathcal{N}(\mathbf{x}; \mathbf{z}_0, \delta^2 I)$, where $\delta^2 = 10^{-4}$.

This particular parameterization of the reverse process is not the only possibility. However, it is a convenient choice as it allows for the definition of the reverse process simply through the prediction of \mathbf{x} , akin to conventional diffusion models (Ho et al., 2020).

3.3. Optimization

We propose to optimize the forward and reverse processes of NFDM jointly, minimizing the following objective:

$$\mathcal{L} = \mathcal{L}_{\text{rec}} + \mathcal{L}_{\text{diff}} + \mathcal{L}_{\text{prior}}, \quad (18)$$

$$\mathcal{L}_{\text{rec}} = \mathbb{E}_{q_\varphi(\mathbf{x}, \mathbf{z}_0)} [-\log p(\mathbf{x} | \mathbf{z}_0)], \quad (19)$$

$$\mathcal{L}_{\text{diff}} = \mathbb{E}_{u(t)q_\varphi(\mathbf{x}, \mathbf{z}_t)} \left[\frac{1}{2g_\varphi^2(t)} \|\tilde{f}_\varphi^B(\mathbf{z}_t, t, \mathbf{x}) - \hat{f}_{\theta, \varphi}(\mathbf{z}_t, t)\|_2^2 \right], \quad (20)$$

$$\mathcal{L}_{\text{prior}} = \mathbb{E}_{q(\mathbf{x})} [\text{D}_{\text{KL}}(q_\varphi(\mathbf{z}_1 | \mathbf{x}) \| p(\mathbf{z}_1))]. \quad (21)$$

Algorithm 1 Optimization of NFDM

Require: $q(x), F_\varphi, \hat{\mathbf{x}}_\theta$

for learning iterations **do**

$\mathbf{x} \sim q(x), t \sim u(t), \{\mathbf{z}_0, \mathbf{z}_t, \mathbf{z}_1\} \sim q(\cdot | \mathbf{x})$

$\mathcal{L}_{\text{rec}} = -\log p(\mathbf{x} | \mathbf{z}_0)$

$\mathcal{L}_{\text{diff}} = \frac{1}{2g_\varphi^2(t)} \|\tilde{f}_\varphi^B(\mathbf{z}_t, t, \mathbf{x}) - \hat{f}_{\theta, \varphi}(\mathbf{z}_t, t)\|_2^2$

$\mathcal{L}_{\text{prior}} = \log q_\varphi(\mathbf{z}_1 | x) - \log p(\mathbf{z}_1)$

Gradient step on θ and φ w.r.t. $\mathcal{L}_{\text{rec}} + \mathcal{L}_{\text{diff}} + \mathcal{L}_{\text{prior}}$

end for

Algorithm 2 Stochastic sampling from NFDM

Require: $F_\varphi, \hat{\mathbf{x}}_\theta, T$ – number of steps

$\Delta t = \frac{1}{T}, \mathbf{z}_1 \sim p(\mathbf{z}_1)$

for $t = 1, \dots, \frac{2}{T}, \frac{1}{T}$ **do**

$\bar{\mathbf{w}} \sim \mathcal{N}(0, I)$

$\mathbf{z}_{t-\Delta t} = \mathbf{z}_t - \hat{f}_{\theta, \varphi}(\mathbf{z}_t, t)\Delta t + g_\varphi(t)\bar{\mathbf{w}}\sqrt{\Delta t}$

end for

$\mathbf{x} \sim p(\mathbf{x} | \mathbf{z}_0)$

As we demonstrate in Appendix A.1 these objectives provide a variational bound on the model’s likelihood $p_{\theta, \varphi}(\mathbf{x})$.

The objective \mathcal{L} shares similarities with the standard diffusion model objective (Ho et al., 2020), though the individual terms differ. Moreover, if the forward process is parameterized by φ , we need to optimize the objective (eq. (18)) with respect to these parameters. The objective \mathcal{L} also exhibits strong connections with both the Flow Matching (Lipman et al., 2022) and Score Matching (Vincent, 2011) objectives. We explore these connections in Appendix B.2, where we also discuss the role of g_φ .

A key characteristic of the NFDM objective is its amenability to training within a simulation-free paradigm, which is critical for efficient optimization. We summarize the training procedure in Algorithm 1.

3.4. Sampling

NFDM offers several methods for sampling from the trained reverse process. The first method is stochastic sampling, as defined in Section 3.2. This process involves the following steps: 1) sample $\mathbf{z}_1 \sim p(\mathbf{z}_1)$; 2) numerically simulate the SDE (eq. (16)) to obtain \mathbf{z}_0 ; 3) sample $\mathbf{x} \sim p(\mathbf{x} | \mathbf{z}_0)$. This procedure is summarized in Algorithm 2.

Moreover, during the sampling process, we can adjust the level of stochasticity by modifying $g_\varphi(t)$ (eq. (12)). It is important to note that changes to $g_\varphi(t)$ also influence \tilde{f}_φ^B (eq. (12)) and $\hat{f}_{\theta, \varphi}$ (eq. (17)). In the extreme case where $g_\varphi(t) \equiv 0$, the reverse process becomes deterministic, allowing us to utilize off-the-shelf numerical ODE solvers

and to estimate densities (Chen et al., 2018a; Grathwohl et al., 2018).

3.5. Parameterization

The parameterization of the variance function $g_\varphi(t)$ (eq. (12)) and the data point predictor $\hat{\mathbf{x}}_\theta(\mathbf{z}_t, t)$ (eq. (17)) is straightforward. In our experiments, we parameterize them directly using neural networks. However, the parameterization of the transformation F_φ (eq. (9)) is more complex. NFDM necessitates that F_φ be differentiable and invertible with respect to ε , as well as provide access to the logarithm of the determinant of the transformation $\log |J_{F_\varphi}^{-1}|$ (eq. (14)). Therefore, we use the following parameterization for F_φ :

$$F_\varphi(\varepsilon, t, \mathbf{x}) = \mu_\varphi(\mathbf{x}, t) + \varepsilon \sigma_\varphi(\mathbf{x}, t), \quad \text{where} \quad (22)$$

$$\mu_\varphi(\mathbf{x}, t) = (1-t)\mathbf{x} + t(1-t)\bar{\mu}_\varphi(\mathbf{x}, t), \quad (23)$$

$$\sigma_\varphi(\mathbf{x}, t) = \delta + t\bar{\sigma}_\varphi((1-t)\mathbf{x}, t) / \bar{\sigma}_\varphi(\mathbf{0}, 1). \quad (24)$$

In this context, $\bar{\mu}_\varphi : \mathbb{R}^D \times [0, 1] \mapsto \mathbb{R}^D$ and $\bar{\sigma}_\varphi : \mathbb{R}^D \times [0, 1] \mapsto \mathbb{R}_+^D$, with δ being a constant. In our experiments, we set $\delta^2 = 10^{-4}$. If $\bar{\mu}_\varphi$ and $\bar{\sigma}_\varphi$ are differentiable, this parameterization meets the requirements on F_φ and renders $q(\mathbf{z}_t|\mathbf{x})$ a conditional Gaussian distribution with parameterized mean and diagonal covariance matrix.

Furthermore, this reparameterization ensures that $q(\mathbf{z}_0|\mathbf{x}) = \mathcal{N}(\mathbf{z}_0; \mathbf{x}, \delta^2 I)$ and $q(\mathbf{z}_1|\mathbf{x}) = \mathcal{N}(\mathbf{z}_1; 0, I)$. These restrictions are not necessary for F_φ , however, it eliminates the need to optimize the reconstruction loss \mathcal{L}_{rec} (eq. (19)) and the prior loss $\mathcal{L}_{\text{prior}}$ (eq. (21)), as they are independent of the parameters φ and θ .

The chosen parameterization of F_φ , $g_\varphi(t)$, and $\hat{\mathbf{x}}_\theta(\mathbf{z}_t, t)$ is not the only possible approach and may not be optimal. For instance, it is possible to parameterize F_φ as a flow-based model (Dinh et al., 2016; Kingma & Dhariwal, 2018), enabling a broader range of distributions than just conditional Gaussians. However, for the purpose of this paper, we maintain a simple setup and leave the exploration of the most effective parameterization for future research.

We discuss the parameterization in more detail in Appendix C.2.

4. Restricted NFDM

We introduce NFDM as a powerful framework that enables both pre-definition and learning of the forward process, potentially simplifying the task for the reverse process. However, there are in general an infinite number of forward and reverse processes that correspond to each other. So how to choose between them? The standard NFDM, as described in Section 3, learns one such pair of processes. However, the flexibility of NFDM opens up the possibility of choos-

ing specific pairs of processes depending on the task.

Suppose our objective is not just to learn any generative process for the data, but to learn one endowed with specific beneficial properties. For instance, one such property is straight generative ODE trajectories. Learning a generative process with straight ODE trajectories can be highly beneficial, as it enables the generation of samples with far fewer steps in the ODE solver. This can lead to significant computational savings.

To achieve this, we must introduce some restrictions on the reverse process. One approach is to directly encode this in the definition of the reverse process. Alternatively, we can introduce penalties on the curvature of its trajectories. In both cases learnable forward process would then adapt to align with the reverse process. As a result, we would obtain a generative process that not only corresponds to the forward process, ensuring accurate data generation, but also features the desired property of straight trajectories. We discuss NFDM with restrictions in more details in Appendix A.2.

Importantly, conventional diffusion models are incapable of handling such constraints or penalization strategies. In diffusion models with a fixed forward process, the target for the reverse process is predetermined and the corresponding ODE trajectories are highly curved. Hence, imposing constraints on the reverse process, such as trajectory straightness, would lead to a mismatch with the forward process and, consequently, an inability to generate samples with high data fidelity.

4.1. NFDM with optimal transport

In this section, we discuss curvature penalization on the ODE trajectories of the reverse process in NFDM. We refer to this variant as NFDM-OT¹.

We propose learning a model with an additional curvature penalty as suggested by Kelly et al. (2020):

$$\mathcal{L}_{\text{OT}} = \mathcal{L} + \lambda \mathcal{L}_{\text{crv}}, \quad \text{where} \quad (25)$$

$$\mathcal{L}_{\text{crv}} = \mathbb{E}_{u(t)q_\varphi(\mathbf{x}, \mathbf{z}_t)} \left\| \frac{d\hat{f}_{\theta, \varphi}(\mathbf{z}_t, t)}{dt} \right\|_2^2. \quad (26)$$

\mathcal{L}_{crv} is an additional curvature loss that penalizes the second time derivative of the generative ODE trajectories. \mathcal{L} is estimated as in section 3.3, whereas when calculating \mathcal{L}_{crv} we set $g_\varphi(t) \equiv 0$. $\mathcal{L}_{\text{crv}} \equiv 0$ ensures that the generative trajectories are straight lines. Although we parameterize $\hat{f}_{\theta, \varphi}$ (eq. (17)) through \tilde{f}_φ^B (eq. (15)), \mathcal{L}_{crv} does not penalize the curvature of the conditional forward trajectories.

¹OT stands for optimal transport. This designation is used for convenience. While straight trajectories are a necessary condition for dynamic optimal transport, they are not sufficient.

Table 1. Comparison of NFDM results with baselines on density estimation tasks. We present results in terms of BPD, lower is better. NFDM achieves state-of-the-art results across the three benchmark tasks.

Model	CIFAR10	ImageNet 32	ImageNet 64
DDPM (Ho et al., 2020)	3.69		
Score SDE (Song et al., 2020b)	2.99		
Improved DDPM (Nichol & Dhariwal, 2021)	2.94		3.54
VDM (Kingma et al., 2021)	2.65	3.72	3.40
Score Flow (Song et al., 2021)	2.83	3.76	
Flow Matching (Lipman et al., 2022)	2.99	3.53	3.31
Stochastic Interp. (Albergo & Vanden-Eijnden, 2022)	2.99	3.48	
i-DODE (Zheng et al., 2023b)	2.56	3.43	
MuLAN (Sahoo et al., 2023)	2.55	3.67	
NFDM (this paper)	2.49	3.36	3.20

The penalty requires F_φ to be twice differentiable with respect to time. The specifics of the curvature loss are elaborated upon in more detail in Appendix A.2.

Even though the parameterization, as discussed in section 3.5, is simple and does not guarantee reaching the zero curvature, we find that in practice it is flexible enough to successfully learn straight line generative trajectories. In our experiments, we set $\lambda = 10^{-2}$. Empirical evidence suggests that higher values of λ lead to slower convergence of the model. We provide empirical results for NFDM-OT in Section 5.2.

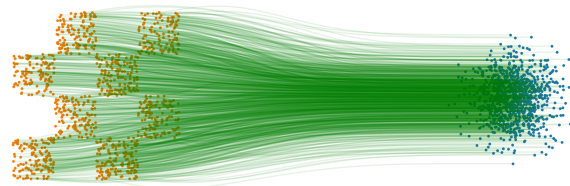
5. Experiments

We first showcase results demonstrating that NFDM consistently achieves better likelihood compared to baselines, obtaining state-of-the-art diffusion modeling results on the CIFAR-10 and downsampled ImageNet datasets. Then, we explore the NFDM-OT modification, which penalizes the curvature of the deterministic generative trajectories. The NFDM-OT reduces trajectory curvature, significantly lowering the number of generative steps required for sampling.

We evaluate NFDM on synthetic data, CIFAR-10 (Krizhevsky et al., 2009), and two downsampled ImageNet (Deng et al., 2009; Van Den Oord et al., 2016) datasets. For parameterization we use multi-layer perceptrons for synthetic data and the U-Net architecture from Dhariwal & Nichol (2021) for images.

We report the NLL in Bits Per Dimension (BPD) and sample quality measured by the FID score (Heusel et al., 2017). The NLL is calculated by integrating the ODEs using the RK45 solver Dormand & Prince (1980), with all NLL metrics computed on test data. For the FID, we provide the average over 50k images.

For a detailed description of parameterizations and other experimental details, please refer to Appendix C.



(a) Score SDE (Song et al., 2020b)



(b) NFDM (this paper)

Figure 1. Comparison of trajectories between the data distribution (on the left) and the prior distribution (on the right).

5.1. Likelihood estimation

We have trained NFDM on the CIFAR-10 and downsampled ImageNet datasets. The NLL results are summarized in Table 1. Notably, NFDM outperforms diffusion-based baselines on all three datasets. We consider this enhanced performance of the NFDM a natural progression due to the following reasons.

First, it is well-established (Song et al., 2021; Zheng et al., 2023b) that diffusion models exhibit improved likelihood estimation when trained with the full ELBO objective. As delineated in Section 3.3, the objective \mathcal{L} (eq. (18)) used for training the NFDM constitutes a variational bound on the likelihood.

Second, as previously mentioned, diffusion models can be seen as hierarchical VAEs. From this perspective, the base-

Table 2. Summary of FID results for few-step generation. The table is divided into three sections, based on different types of methods: those that do not minimize curvature, solvers for pretrained models, and models that specifically aim to minimize curvature. For the DDPM, we include results corresponding to two distinct objectives: the full ELBO-based objective and a simplified objective ($\mathcal{L}_{\text{simple}}$). NFDM-OT outperforms baselines with comparable NFE values.

Model	CIFAR-10		ImageNet 32		ImageNet 64	
	NFE ↓	FID ↓	NFE ↓	FID ↓	NFE ↓	FID ↓
DDPM ($\mathcal{L}_{\text{simple}}$) (Ho et al., 2020)	1000	3.17				
DDPM (ELBO) (Ho et al., 2020)	1000	13.51				
Flow Matching (Lipman et al., 2022)	142	6.35	122	5.02	138	14.14
DDIM (Song et al., 2020a)	10	13.36				
DPM Solver (Lu et al., 2022)	12	5.28				
	24	2.75				
Trajectory Curvature Minimization (Lee et al., 2023)	5	18.74				
Multisample Flow Matching (Pooladian et al., 2023)			4	17.28	4	38.45
			12	7.18	12	17.6
	2	12.44	2	9.83	2	27.70
NFDM-OT (this paper)	4	7.76	4	6.13	4	17.28
	12	5.20	12	4.11	12	11.58

lines in Table 1 resemble VAEs with either fixed or constrained variational distributions. In contrast, the NFDM extends beyond these baselines by providing a more flexible variational distribution. This flexibility allows the NFDM to better conform to the reverse process, consequently enhancing likelihood estimation.

5.2. Straight trajectories

We next evaluate NFDM-OT, which is designed to penalize the curvature of deterministic generative trajectories. Initially, we compare NFDM-OT with a conventional continuous-time diffusion model. Figure 1a illustrates deterministic trajectories between a two-dimensional data distribution and a unit Gaussian distribution learnt by a conventional diffusion model (Song et al., 2020b). Figure 1b depicts trajectories learnt by NFDM-OT. Conventional diffusion, being constrained in its forward process, learns highly curved trajectories, whereas NFDM-OT successfully learns straight generative trajectories as desired.

Subsequently, we present evaluation results of NFDM-OT on image datasets. Table 2 reports the FID scores for 2, 4, and 12 Number of Function Evaluations (NFE) with respect to the function $f_{\theta, \varphi}$ (eq. (16)). In this experiment, we employ Euler’s method for sampling integration. For the specified NFEs, NFDM-OT demonstrates superior sample quality compared to other approaches with similar NFE values. Specifically, NFDM-OT outperforms approaches that minimize the curvature of generative trajectories (Pooladian et al., 2023; Lee et al., 2023).

Importantly, NFDM-OT is trained with an ELBO-based

objective (eq. (18)), which is known to yield higher FID scores for diffusion models (Song et al., 2021; Zheng et al., 2023b). In contrast, some of the approaches listed in Table 2 are trained with different objectives, leading to improved FID scores. Even so, for comparable NFE values NFDM-OT still achieves superior results.

The primary aim of the experiments with NFDM-OT is not to introduce a novel model that surpasses others in few-step generation, but rather to showcase NFDM’s ability to learn generative dynamics with specific properties. The straightness of the trajectories is just one example of such properties. We leave it for future research to explore different parameterizations and a modified objectives for NFDM that may yield even better results.

6. Related work

Diffusion models, originally proposed by Sohl-Dickstein et al. (2015), have evolved significantly through subsequent developments (Song & Ermon, 2019; Ho et al., 2020). These advancements have resulted in remarkable generative quality for high-dimensional data distributions (Dhariwal & Nichol, 2021; Saharia et al., 2022). Nevertheless, conventional diffusion models, typically relying on a linear Gaussian forward process, may not optimally fit some data distributions. To address this, alternative forward processes have been explored, such as combining blurring with Gaussian noise injection (Rissanen et al., 2022; Daras et al., 2022; Hoogeboom & Salimans, 2022), diffusion in the wavelet spectrum (Phung et al., 2023), and forward processes based on the exponential family (Okhotin et al., 2023). These models are limited by their fixed forward pro-

cesses and may be seen as specific instances of NFDM.

Some studies have focused on making the forward process learnable. Approaches include a learnable noise injection schedule (Kingma et al., 2021; Nichol & Dhariwal, 2021; Sahoo et al., 2023) and learning data transformations like time-independent transformations based on VAEs (Vahdat et al., 2021; Rombach et al., 2022) and normalizing flows (Kim et al., 2022), or time-dependent transformations (Gu et al., 2022; Nielsen et al., 2023; Bartosh et al., 2023). These methods can also be considered special cases of NFDM with specific transformations F_φ (eq. (9)).

Recent studies (Zhang & Chen, 2021; De Bortoli et al., 2021; Shi et al., 2023) have explored generative models based on Schrödinger Bridge theory and finite-time diffusion constructions. While these models offer novel approaches to learning forward transformations, in contrast to NFDM, they depart from the simulation-free paradigm by requiring the full simulation of the stochastic processes for training, increasing their computational cost.

Despite the simulation-free nature of the training procedure, diffusion models still necessitate full reverse process simulations for sample generation, leading to slow and computationally expensive inference. To address this, in an orthogonal line of works alternative sampling methods have been studied, such as deterministic sampling in discrete (Song et al., 2020a) and continuous time (Song et al., 2020b) and novel numerical solvers (Tachibana et al., 2021; Liu et al., 2022a; Lu et al., 2022; Shaul et al., 2023b). Additionally, distillation techniques have been applied to both discrete (Salimans & Ho, 2022) and continuous time models (Song et al., 2023; Zheng et al., 2023a; Yin et al., 2023) to enhance sampling speed, albeit at the cost of training additional models. Most of these approaches are compatible with NFDM and may be combined for further gains.

The significance of deterministic trajectories in efficient sampling was highlighted by Karras et al. (2022). At the same time, building on diffusion model concepts, Lipman et al. (2022); Liu et al. (2022b); Albergo & Vanden-Eijnden (2022) introduced simulation-free methods for learning deterministic generative dynamics. Based on these ideas, Liu et al. (2022b) and Liu (2022) proposed distillation procedures to straighten deterministic generative trajectories. Since these methods are based on distillation, we consider them orthogonal to NFDM.

Pooladian et al. (2023) and Tong et al. (2023) proposed to construct the forward process with optimal data-noise couplings to learn straighter generative trajectories. While this method is theoretically justified, it relies on estimating an optimal coupling over minibatches of the entire dataset, which, for large datasets, may become uninformative as to the true coupling. In contrast, NFDM-OT directly penal-

izes curvature of generative trajectories.

Lee et al. (2023) suggested learning the forward process distribution $q(\mathbf{z}_1|\mathbf{x})$ and interpolating linearly between \mathbf{x} and \mathbf{z}_1 . Similarly, Shaul et al. (2023a) aimed to modify the forward process to reduce curvature in the generative process. Both approaches can be viewed as specific instances of NFDM.

Lastly, Albergo et al. (2023) suggested optimizing the forward process simultaneously to training the reverse process, resulting in a challenging high dimensional min-max problem. Moreover, only the theoretical algorithm was presented, without empirical study and descriptions of ways to parameterize such a learnable forward process.

We continue discussing related works in Appendix B.

7. Discussion and Limitations

In this paper we introduced NFDM, a novel simulation-free framework for improved diffusion modeling through a learnable forward processes. Our approach outperforms baseline diffusion models on standard benchmarks, showcasing the effectiveness of NFDM in log-likelihood estimation.

We introduce NFDM not merely as a specific model, but rather as a versatile framework that facilitates the predefined specification and learning of the forward process. For the sake of simplicity in this work, we have chosen a straightforward Gaussian parameterization for the forward process (see Section 3.5). However, NFDM is capable of supporting far more flexible parameterizations beyond standard Gaussian distributions.

Similarly, the penalty on the curvature of deterministic trajectories discussed in Section 4.1 represents just one specific example of the restrictions that NFDM can accommodate. NFDM opens up significant prospects for exploring new generative dynamics.

Nonetheless, the advantages of NFDM come with certain trade-offs. Once the forward process is parameterized using a neural network, this leads to increased computational costs compared to conventional diffusion models. In our experiments, an optimization iteration of NFDM takes approximately 2.2 times longer than that of conventional diffusion models.

Despite these challenges, we are optimistic about the potential of NFDM in various domains and practical applications, given its flexibility in learning generative processes. We also believe that with alternative parameterizations, modifications of the objective, and the integration of orthogonal approaches like distillation, NFDM has the potential to achieve even better results.

References

- Albergo, M. S. and Vanden-Eijnden, E. Building normalizing flows with stochastic interpolants. *arXiv preprint arXiv:2209.15571*, 2022.
- Albergo, M. S., Boffi, N. M., and Vanden-Eijnden, E. Stochastic interpolants: A unifying framework for flows and diffusions. *arXiv preprint arXiv:2303.08797*, 2023.
- Anderson, B. D. Reverse-time diffusion equation models. *Stochastic Processes and their Applications*, 12(3):313–326, 1982.
- Bartosh, G., Vetrov, D., and Naesseth, C. A. Neural diffusion models. *arXiv preprint arXiv:2310.08337*, 2023.
- Bradbury, J., Frostig, R., Hawkins, P., Johnson, M. J., Leary, C., Maclaurin, D., Necula, G., Paszke, A., VanderPlas, J., Wanderman-Milne, S., and Zhang, Q. JAX: composable transformations of Python+NumPy programs, 2018. URL <http://github.com/google/jax>.
- Chen, R. T., Rubanova, Y., Bettencourt, J., and Duvenaud, D. K. Neural ordinary differential equations. *Advances in neural information processing systems*, 31, 2018a.
- Chen, Z., Yeo, C. K., Lee, B. S., and Lau, C. T. Autoencoder-based network anomaly detection. In *2018 Wireless telecommunications symposium (WTS)*, pp. 1–5. IEEE, 2018b.
- Creswell, A., White, T., Dumoulin, V., Arulkumaran, K., Sengupta, B., and Bharath, A. A. Generative adversarial networks: An overview. *IEEE Signal Processing Magazine*, 35(1):53–65, 2018.
- Daras, G., Delbraccio, M., Talebi, H., Dimakis, A. G., and Milanfar, P. Soft diffusion: Score matching for general corruptions. *arXiv preprint arXiv:2209.05442*, 2022.
- De Bortoli, V., Thornton, J., Heng, J., and Doucet, A. Diffusion schrödinger bridge with applications to score-based generative modeling. *Advances in Neural Information Processing Systems*, 34:17695–17709, 2021.
- Deng, J., Dong, W., Socher, R., Li, L.-J., Li, K., and Fei-Fei, L. Imagenet: A large-scale hierarchical image database. In *2009 IEEE conference on computer vision and pattern recognition*, pp. 248–255. Ieee, 2009.
- Dhariwal, P. and Nichol, A. Diffusion models beat GANs on image synthesis. *arXiv preprint arXiv:2105.05233*, 2021.
- Dias, M. L., Mattos, C. L. C., da Silva, T. L., de Macedo, J. A. F., and Silva, W. C. Anomaly detection in trajectory data with normalizing flows. In *2020 international joint conference on neural networks (IJCNN)*, pp. 1–8. IEEE, 2020.
- Dinh, L., Sohl-Dickstein, J., and Bengio, S. Density estimation using real nvp. *arXiv preprint arXiv:1605.08803*, 2016.
- Dormand, J. R. and Prince, P. J. A family of embedded runge-kutta formulae. *Journal of computational and applied mathematics*, 6(1):19–26, 1980.
- Grathwohl, W., Chen, R. T., Bettencourt, J., Sutskever, I., and Duvenaud, D. Ffjord: Free-form continuous dynamics for scalable reversible generative models. *arXiv preprint arXiv:1810.01367*, 2018.
- Gu, J., Zhai, S., Zhang, Y., Bautista, M. A., and Susskind, J. f-dm: A multi-stage diffusion model via progressive signal transformation. *arXiv preprint arXiv:2210.04955*, 2022.
- Heusel, M., Ramsauer, H., Unterthiner, T., Nessler, B., and Hochreiter, S. Gans trained by a two time-scale update rule converge to a local nash equilibrium. *Advances in neural information processing systems*, 30, 2017.
- Ho, J., Jain, A., and Abbeel, P. Denoising diffusion probabilistic models. *arXiv preprint arXiv:2006.11239*, 2020.
- Ho, J., Saharia, C., Chan, W., Fleet, D. J., Norouzi, M., and Salimans, T. Cascaded diffusion models for high fidelity image generation. *The Journal of Machine Learning Research*, 23(1):2249–2281, 2022.
- Ho, Y.-H., Chan, C.-C., Peng, W.-H., Hang, H.-M., and Domański, M. Anfic: Image compression using augmented normalizing flows. *IEEE Open Journal of Circuits and Systems*, 2:613–626, 2021.
- Hoogeboom, E. and Salimans, T. Blurring diffusion models. *arXiv preprint arXiv:2209.05557*, 2022.
- Karras, T., Aittala, M., Aila, T., and Laine, S. Elucidating the design space of diffusion-based generative models. *Advances in Neural Information Processing Systems*, 35: 26565–26577, 2022.
- Kelly, J., Bettencourt, J., Johnson, M. J., and Duvenaud, D. K. Learning differential equations that are easy to solve. *Advances in Neural Information Processing Systems*, 33:4370–4380, 2020.
- Kim, D., Na, B., Kwon, S. J., Lee, D., Kang, W., and Moon, I.-C. Maximum likelihood training of implicit nonlinear diffusion models. *arXiv preprint arXiv:2205.13699*, 2022.

- Kingma, D. P. and Dhariwal, P. Glow: Generative flow with invertible 1x1 convolutions. *Advances in neural information processing systems*, 31, 2018.
- Kingma, D. P. and Welling, M. Auto-encoding variational Bayes. *arXiv preprint arXiv:1312.6114*, 2013.
- Kingma, D. P., Salimans, T., Poole, B., and Ho, J. Variational diffusion models. *arXiv preprint arXiv:2107.00630*, 2, 2021.
- Krizhevsky, A., Hinton, G., et al. Learning multiple layers of features from tiny images. 2009.
- Lee, S., Kim, B., and Ye, J. C. Minimizing trajectory curvature of ode-based generative models. *arXiv preprint arXiv:2301.12003*, 2023.
- Lipman, Y., Chen, R. T., Ben-Hamu, H., Nickel, M., and Le, M. Flow matching for generative modeling. *arXiv preprint arXiv:2210.02747*, 2022.
- Liu, L., Ren, Y., Lin, Z., and Zhao, Z. Pseudo numerical methods for diffusion models on manifolds. *arXiv preprint arXiv:2202.09778*, 2022a.
- Liu, Q. Rectified flow: A marginal preserving approach to optimal transport. *arXiv preprint arXiv:2209.14577*, 2022.
- Liu, X., Gong, C., and Liu, Q. Flow straight and fast: Learning to generate and transfer data with rectified flow. *arXiv preprint arXiv:2209.03003*, 2022b.
- Lu, C., Zhou, Y., Bao, F., Chen, J., Li, C., and Zhu, J. Dpm-solver: A fast ode solver for diffusion probabilistic model sampling in around 10 steps. *Advances in Neural Information Processing Systems*, 35:5775–5787, 2022.
- Nichol, A. and Dhariwal, P. Improved denoising diffusion probabilistic models. *arXiv preprint arXiv:2102.09672*, 2021.
- Nielsen, B. M., Christensen, A., Dittadi, A., and Winther, O. Diffenc: Variational diffusion with a learned encoder. *arXiv preprint arXiv:2310.19789*, 2023.
- Okhotin, A., Molchanov, D., Arkhipkin, V., Bartosh, G., Alanov, A., and Vetrov, D. Star-shaped denoising diffusion probabilistic models. *arXiv preprint arXiv:2302.05259*, 2023.
- Papamakarios, G., Nalisnick, E., Rezende, D. J., Mohamed, S., and Lakshminarayanan, B. Normalizing flows for probabilistic modeling and inference. *The Journal of Machine Learning Research*, 22(1):2617–2680, 2021.
- Paszke, A., Gross, S., Chintala, S., Chanan, G., Yang, E., DeVito, Z., Lin, Z., Desmaison, A., Antiga, L., and Lerer, A. Automatic differentiation in pytorch. 2017.
- Phung, H., Dao, Q., and Tran, A. Wavelet diffusion models are fast and scalable image generators. In *Proceedings of the IEEE/CVF Conference on Computer Vision and Pattern Recognition*, pp. 10199–10208, 2023.
- Pooladian, A.-A., Ben-Hamu, H., Domingo-Enrich, C., Amos, B., Lipman, Y., and Chen, R. Multisample flow matching: Straightening flows with minibatch couplings. *arXiv preprint arXiv:2304.14772*, 2023.
- Rezende, D. J., Mohamed, S., and Wierstra, D. Stochastic backpropagation and approximate inference in deep generative models. In *International conference on machine learning*, pp. 1278–1286. PMLR, 2014.
- Rissanen, S., Heinonen, M., and Solin, A. Generative modelling with inverse heat dissipation. *arXiv preprint arXiv:2206.13397*, 2022.
- Rombach, R., Blattmann, A., Lorenz, D., Esser, P., and Ommer, B. High-resolution image synthesis with latent diffusion models. In *Proceedings of the IEEE/CVF conference on computer vision and pattern recognition*, pp. 10684–10695, 2022.
- Saharia, C., Chan, W., Saxena, S., Li, L., Whang, J., Denton, E. L., Ghasemipour, K., Gontijo Lopes, R., Karagol Ayan, B., Salimans, T., et al. Photorealistic text-to-image diffusion models with deep language understanding. *Advances in Neural Information Processing Systems*, 35:36479–36494, 2022.
- Sahoo, S. S., Gokaslan, A., De Sa, C., and Kuleshov, V. Diffusion models with learned adaptive noise. *arXiv preprint arXiv:2312.13236*, 2023.
- Salimans, T. and Ho, J. Progressive distillation for fast sampling of diffusion models. *arXiv preprint arXiv:2202.00512*, 2022.
- Serrà, J., Álvarez, D., Gómez, V., Slizovskaia, O., Núñez, J. F., and Luque, J. Input complexity and out-of-distribution detection with likelihood-based generative models. *arXiv preprint arXiv:1909.11480*, 2019.
- Shaul, N., Chen, R. T., Nickel, M., Le, M., and Lipman, Y. On kinetic optimal probability paths for generative models. In *International Conference on Machine Learning*, pp. 30883–30907. PMLR, 2023a.
- Shaul, N., Perez, J., Chen, R. T., Thabet, A., Pumarola, A., and Lipman, Y. Bespoke solvers for generative flow models. *arXiv preprint arXiv:2310.19075*, 2023b.

- Shi, Y., De Bortoli, V., Campbell, A., and Doucet, A. Diffusion schrödinger bridge matching. *arXiv preprint arXiv:2303.16852*, 2023.
- Sohl-Dickstein, J., Weiss, E., Maheswaranathan, N., and Ganguli, S. Deep unsupervised learning using nonequilibrium thermodynamics. In *International Conference on Machine Learning*, pp. 2256–2265. PMLR, 2015.
- Song, J., Meng, C., and Ermon, S. Denoising diffusion implicit models. *arXiv preprint arXiv:2010.02502*, 2020a.
- Song, Y. and Ermon, S. Generative modeling by estimating gradients of the data distribution. *arXiv preprint arXiv:1907.05600*, 2019.
- Song, Y., Sohl-Dickstein, J., Kingma, D. P., Kumar, A., Ermon, S., and Poole, B. Score-based generative modeling through stochastic differential equations. *arXiv preprint arXiv:2011.13456*, 2020b.
- Song, Y., Durkan, C., Murray, I., and Ermon, S. Maximum likelihood training of score-based diffusion models. *Advances in Neural Information Processing Systems*, 34: 1415–1428, 2021.
- Song, Y., Dhariwal, P., Chen, M., and Sutskever, I. Consistency models. *arXiv preprint arXiv:2303.01469*, 2023.
- Tachibana, H., Go, M., Inahara, M., Katayama, Y., and Watanabe, Y. Itô-taylor sampling scheme for denoising diffusion probabilistic models using ideal derivatives. *arXiv preprint arXiv:2112.13339*, 2021.
- Tan, X., Chen, J., Liu, H., Cong, J., Zhang, C., Liu, Y., Wang, X., Leng, Y., Yi, Y., He, L., et al. Naturalspeech: End-to-end text-to-speech synthesis with human-level quality. *IEEE Transactions on Pattern Analysis and Machine Intelligence*, 2024.
- Tomczak, J. M. *Deep generative modeling*. Springer, 2022.
- Tong, A., Malkin, N., Huguet, G., Zhang, Y., Rector-Brooks, J., Fatras, K., Wolf, G., and Bengio, Y. Improving and generalizing flow-based generative models with minibatch optimal transport. In *ICML Workshop on New Frontiers in Learning, Control, and Dynamical Systems*, 2023.
- Trippe, B. L., Yim, J., Tischer, D., Baker, D., Broderick, T., Barzilay, R., and Jaakkola, T. S. Diffusion probabilistic modeling of protein backbones in 3D for the motif-scaffolding problem. In *The Eleventh International Conference on Learning Representations*, 2023.
- Vahdat, A., Kreis, K., and Kautz, J. Score-based generative modeling in latent space. *Advances in Neural Information Processing Systems*, 34:11287–11302, 2021.
- Van Den Oord, A., Kalchbrenner, N., and Kavukcuoglu, K. Pixel recurrent neural networks. In *International conference on machine learning*, pp. 1747–1756. PMLR, 2016.
- Vincent, P. A connection between score matching and denoising autoencoders. *Neural computation*, 23(7):1661–1674, 2011.
- Watson, J. L., Juergens, D., Bennett, N. R., Trippe, B. L., Yim, J., Eisenach, H. E., Ahern, W., Borst, A. J., Ragotte, R. J., Milles, L. F., et al. De novo design of protein structure and function with rfdiffusion. *Nature*, 620(7976):1089–1100, 2023.
- Xiao, Z., Yan, Q., and Amit, Y. Likelihood regret: An out-of-distribution detection score for variational autoencoder. *Advances in neural information processing systems*, 33:20685–20696, 2020.
- Yang, L., Zhang, Z., Song, Y., Hong, S., Xu, R., Zhao, Y., Shao, Y., Zhang, W., Cui, B., and Yang, M.-H. Diffusion models: A comprehensive survey of methods and applications. *arXiv preprint arXiv:2209.00796*, 2022.
- Yang, R. and Mandt, S. Lossy image compression with conditional diffusion models. *arXiv preprint arXiv:2209.06950*, 2022.
- Yin, T., Gharbi, M., Zhang, R., Shechtman, E., Durand, F., Freeman, W. T., and Park, T. One-step diffusion with distribution matching distillation. *arXiv preprint arXiv:2311.18828*, 2023.
- Zhang, Q. and Chen, Y. Diffusion normalizing flow. *arXiv preprint arXiv:2110.07579*, 2021.
- Zheng, H., Nie, W., Vahdat, A., Aizzadenesheli, K., and Anandkumar, A. Fast sampling of diffusion models via operator learning. In *International Conference on Machine Learning*, pp. 42390–42402. PMLR, 2023a.
- Zheng, K., Lu, C., Chen, J., and Zhu, J. Improved techniques for maximum likelihood estimation for diffusion odes. *arXiv preprint arXiv:2305.03935*, 2023b.

A. Derivations

A.1. Derivation of objective

For the forward process, we have the conditional marginal distribution $q_\varphi(\mathbf{z}_t|\mathbf{x})$, which is implicitly defined by the invertible transformation $\mathbf{z}_t = F_\varphi(\varepsilon, t, \mathbf{x})$ (eq. (9)), where $\varepsilon \sim q(\varepsilon)$. Additionally, there's a SDE (eq. (15)) starting from $\mathbf{z}_1 \sim q(\mathbf{z}_1|\mathbf{x})$ and flowing backwards in time:

$$d\mathbf{z}_t = \tilde{f}_\varphi^B(\mathbf{z}_t, t, \mathbf{x})dt + g_\varphi(t)d\mathbf{w}. \quad (27)$$

This SDE corresponds to the marginal distribution $q_\varphi(\mathbf{z}_t|\mathbf{x})$.

The reverse process involves a prior distribution $p(\mathbf{z}_1)$ and a reverse SDE (eq. (15)):

$$d\mathbf{z}_t = \hat{f}_{\theta, \varphi}(\mathbf{z}_t, t)dt + g_\varphi(t)d\bar{\mathbf{w}}. \quad (28)$$

Our goal is to derive a variational bound on the negative log-likelihood of the model.

We begin by discretizing the conditional reverse SDE in eq. (27) and the reverse SDE in eq. (28), transitioning from continuous-time trajectories $\{\mathbf{z}(t)\}_{t \in [0, 1]}$ to discrete-time trajectories $\bar{\mathbf{z}}_0, \bar{\mathbf{z}}_{\frac{1}{T}}, \dots, \bar{\mathbf{z}}_1$, where T represents the number of discrete steps. For convenience, we also introduce $\Delta t = \frac{1}{T}$.

The discretization of the conditional reverse SDE is as follows:

$$\bar{q}_\varphi(\bar{\mathbf{z}}_1|\mathbf{x}) = q_\varphi(\bar{\mathbf{z}}_1|\mathbf{x}), \quad \bar{q}_\varphi(\bar{\mathbf{z}}_{t-\Delta t}|\bar{\mathbf{z}}_t, \mathbf{x}) = \mathcal{N}\left(\bar{\mathbf{z}}_{t-\Delta t}; \bar{\mathbf{z}}_t - \Delta t \tilde{f}_\varphi^B(\bar{\mathbf{z}}_t, t, \mathbf{x}), \Delta t g_\varphi^2(t)I\right). \quad (29)$$

We similarly discretize the reverse SDE:

$$\bar{p}(\bar{\mathbf{z}}_1) = p(\bar{\mathbf{z}}_1), \quad \bar{p}(\mathbf{x}|\bar{\mathbf{z}}_0) = p(\mathbf{x}|\bar{\mathbf{z}}_0), \quad \bar{p}_{\theta, \varphi}(\bar{\mathbf{z}}_{t-\Delta t}|\bar{\mathbf{z}}_t) = \mathcal{N}\left(\bar{\mathbf{z}}_{t-\Delta t}; \bar{\mathbf{z}}_t - \Delta t \hat{f}_{\theta, \varphi}(\bar{\mathbf{z}}_t, t), \Delta t g_\varphi^2(t)I\right). \quad (30)$$

It's important to note that once we discretize the trajectories, $\bar{q}_\varphi(\bar{\mathbf{z}}_t|\mathbf{x}) \neq q_\varphi(\bar{\mathbf{z}}_t|\mathbf{x})$ and $\bar{p}_{\theta, \varphi}(\bar{\mathbf{z}}_t) \neq p_{\theta, \varphi}(\bar{\mathbf{z}}_t)$ except for $t = 1$. However, this discretization corresponds to an Euler-Maruyama method of integrating SDEs. Thus, we know that as $\Delta t \rightarrow 0$, the discretized trajectories converge to the continuous ones.

Now, considering these discrete processes and recognizing that they are Markovian conditional and unconditional processes moving backwards in time, we can leverage a key result from [Ho et al. \(2020\)](#):

$$\mathbb{E}_{q(\mathbf{x})} [-\log \bar{p}_{\theta, \varphi}(\mathbf{x})] \leq \bar{\mathcal{L}}_{\text{recon}} + \bar{\mathcal{L}}_{\text{diff}} + \bar{\mathcal{L}}_{\text{prior}}, \quad \text{where} \quad (31)$$

$$\bar{\mathcal{L}}_{\text{recon}} = \mathbb{E}_{\bar{q}_\varphi(\mathbf{x}, \bar{\mathbf{z}}_0)} [-\log p(\mathbf{x}|\bar{\mathbf{z}}_0)], \quad (32)$$

$$\bar{\mathcal{L}}_{\text{diff}} = \sum_{t=\frac{1}{T}}^T \mathbb{E}_{\bar{q}_\varphi(\mathbf{x}, \bar{\mathbf{z}}_t)} [\text{D}_{\text{KL}}(\bar{q}_\varphi(\bar{\mathbf{z}}_{t-\Delta t}|\bar{\mathbf{z}}_t, \mathbf{x}) \|\bar{p}_{\theta, \varphi}(\bar{\mathbf{z}}_{t-\Delta t}|\bar{\mathbf{z}}_t))], \quad (33)$$

$$\bar{\mathcal{L}}_{\text{prior}} = \mathbb{E}_{q(\mathbf{x})} [\text{D}_{\text{KL}}(\bar{q}_\varphi(\bar{\mathbf{z}}_1|\mathbf{x}) \|\bar{p}(\bar{\mathbf{z}}_1))]. \quad (34)$$

Consequently, eq. (31) establishes a variational upper bound on the negative log-likelihood of discretized reverse process. Taking the limits of this upper bound, the reconstruction term $\bar{\mathcal{L}}_{\text{recon}}$ and the prior term $\bar{\mathcal{L}}_{\text{prior}}$ retain their forms.

However, we can reformulate the diffusion term:

$$\mathcal{L}_{\text{diff}} = \lim_{\Delta t \rightarrow 0} \bar{\mathcal{L}}_{\text{diff}} \quad (35)$$

$$= \lim_{\Delta t \rightarrow 0} \sum_{t=\frac{1}{T}}^T \mathbb{E}_{\bar{q}_\varphi(\mathbf{x}, \bar{\mathbf{z}}_t)} [\text{D}_{\text{KL}}(\bar{q}_\varphi(\bar{\mathbf{z}}_{t-\Delta t} | \bar{\mathbf{z}}_t, \mathbf{x}) \| \bar{p}_{\theta, \varphi}(\bar{\mathbf{z}}_{t-\Delta t} | \bar{\mathbf{z}}_t))] \quad (36)$$

$$= \lim_{\Delta t \rightarrow 0} \sum_{t=\frac{1}{T}}^T \mathbb{E}_{\bar{q}_\varphi(\mathbf{x}, \bar{\mathbf{z}}_t)} \left[\frac{1}{2\Delta t g_\varphi^2(t)} \left\| \bar{\mathbf{z}}_t - \Delta t \hat{f}_{\theta, \varphi}(\bar{\mathbf{z}}_t, t) - \bar{\mathbf{z}}_t + \Delta t \tilde{f}_\varphi^B(\bar{\mathbf{z}}_t, t, \mathbf{x}) \right\|_2^2 \right] \quad (37)$$

$$= \lim_{\Delta t \rightarrow 0} \sum_{t=\frac{1}{T}}^T \mathbb{E}_{\bar{q}_\varphi(\mathbf{x}, \bar{\mathbf{z}}_t)} \left[\frac{\Delta t^2}{2\Delta t g_\varphi^2(t)} \left\| \tilde{f}_\varphi^B(\bar{\mathbf{z}}_t, t, \mathbf{x}) - \hat{f}_{\theta, \varphi}(\bar{\mathbf{z}}_t, t) \right\|_2^2 \right] \quad (38)$$

$$= \mathbb{E}_{u(t)\bar{q}_\varphi(\mathbf{x}, \bar{\mathbf{z}}_t)} \left[\frac{1}{2g_\varphi^2(t)} \left\| \tilde{f}_\varphi^B(\bar{\mathbf{z}}_t, t, \mathbf{x}) - \hat{f}_{\theta, \varphi}(\bar{\mathbf{z}}_t, t) \right\|_2^2 \right], \quad (39)$$

where $u(t)$ is a uniform distribution over a unit interval.

Therefore, as the discretized trajectory tends to the continuous one when $\Delta t \rightarrow 0$, we can use the obtained limits as a variational bound on the negative log-likelihood of the continuous model.

A.2. NFDM with restrictions

In Section 4, we discussed training the NFDM with restrictions on the reverse process. This section aims to explore the limitations of such restrictions and to further discuss the training of NFDM with curvature penalties.

When training NFDM with certain restrictions, it is crucial that these restrictions are feasible. For example, imposing overly stringent constraints on the reverse process (such as fixing its drift term $\hat{f} \equiv 0$) will render the forward process incapable of adapting, regardless of its flexibility. Similarly, unattainable penalties, like those on the squared norm of the drift term $\|\hat{f}_{\theta, \varphi}\|_2^2$, will lead to biased solutions, as it's impossible to match two processes when $\|\hat{f}_{\theta, \varphi}\|_2^2 \equiv 0$.

Hence, in Section 4.1, we suggest penalizing the curvature of deterministic generative trajectories specifically with penalty \mathcal{L}_{crv} (eq. (26)). This is because for non-degenerate data distributions, there exist mappings that transform them into unit Gaussian noise along straight line trajectories.

To calculate the curvature penalty \mathcal{L}_{crv} (eq. (26)), we proceed as follows. First, we use the chain rule to rewrite the time derivative:

$$\frac{d\hat{f}_{\theta, \varphi}(\mathbf{z}_t, t)}{dt} = \frac{\partial \hat{f}_{\theta, \varphi}(\mathbf{z}_t, t)}{\partial \mathbf{z}_t} \frac{\partial \mathbf{z}_t}{\partial t} + \frac{\partial \hat{f}_{\theta, \varphi}(\mathbf{z}_t, t)}{\partial t} \quad (40)$$

$$= \frac{\partial \hat{f}_{\theta, \varphi}(\mathbf{z}_t, t)}{\partial \mathbf{z}_t} \hat{f}_{\theta, \varphi}(\mathbf{z}_t, t) + \frac{\partial \hat{f}_{\theta, \varphi}(\mathbf{z}_t, t)}{\partial t}. \quad (41)$$

The second term in eq. (41) is the time derivative of a function. As discussed in section 3.1, the time derivatives can be determined as a Jacobian Vector Product (JVP) with a one-dimensional unit vector. Notably, the first term in eq. (41) is also a JVP. Therefore, we can combine these two operations. For this purpose, we define a \mathbb{R}^{D+1} dimensional adjoint vector v :

$$v = \begin{bmatrix} \hat{f}_{\theta, \varphi}(\mathbf{z}_t, t) \\ 1 \end{bmatrix}. \quad (42)$$

Consequently, \mathcal{L}_{crv} can be computed as the JVP of $\hat{f}_{\theta, \varphi}(\mathbf{z}_t, t)$ with the vector v .

B. Connections of NFDM with other approaches

B.1. Special cases of NFDM

Many existing works define the forward process in diffusion models as either fixed or simply parameterized processes. These processes can be considered special cases of NFDM. In this section, we review some of these approaches.

Soft Diffusion. Daras et al. (2022) consider a more general case of fixed forward processes, $q(\mathbf{z}_t|\mathbf{x}) = \mathcal{N}(\mathbf{z}_t; C_t\mathbf{x}, \sigma_t I)$, which can be parameterized as $F(\varepsilon, t, \mathbf{x}) = C_t\mathbf{x} + \sigma_t\varepsilon$. Such distributions include, for example, combinations of blurring and the injection of Gaussian noise.

Star-Shaped Diffusion. Okhotin et al. (2023) extended conventional diffusion models to include distributions from the exponential family. Although Star-Shaped Diffusion is a discrete-time approach and does not directly correspond to NFDM, the latter can work with exponential family distributions through reparameterization functions. For instance, for some continuous one-dimensional distribution $q(\mathbf{z}_t|\mathbf{x})$, NFDM could use $F(\varepsilon, t, \mathbf{x}) = a(b(\varepsilon), t, \mathbf{x})$, where a is the inverse Cumulative Distribution Function (CDF) of $q(\mathbf{z}_t|\mathbf{x})$, and b is the CDF of a unit Gaussian.

Variational Diffusion Models. Kingma et al. (2021) proposed forward conditional distributions $q_\varphi(\mathbf{z}_t|\mathbf{x})$ as $\mathcal{N}(\mathbf{z}_t; \alpha_\varphi(t)\mathbf{x}, \sigma_\varphi^2(t)I)$ with learnable parameters φ . In the context of NFDM, this distribution can be parameterized by $F_\varphi(\varepsilon, t, \mathbf{x}) = \alpha_\varphi(t)\mathbf{x} + \sigma_\varphi(t)\varepsilon$.

LSGM. Vahdat et al. (2021) suggest an alternative approach for parameterizing the forward process, proposing diffusion in a latent space of a VAE. Therefore, the forward process is characterized by a distribution $q_\varphi(\mathbf{z}_t|\mathbf{x}) = \mathcal{N}(\mathbf{z}_t; \alpha_t E_\varphi(\mathbf{x}), \sigma_t^2 I)$, where E_φ is the encoder of the VAE. To parameterize the same forward process with NFDM, one could use $F_\varphi(\varepsilon, t, \mathbf{x}) = \alpha_t E_\varphi(\mathbf{x}) + \sigma_t\varepsilon$. To align the reverse process, the reconstruction distribution should be $p(\mathbf{x}|\mathbf{z}_0) = \mathcal{N}(\mathbf{x}; D_\varphi(\mathbf{z}_0), \delta^2 I)$, where D_φ is VAE’s decoder.

DiffEnc. Nielsen et al. (2023) proposed a more general forward process, $q_\varphi(\mathbf{z}_t|\mathbf{x}) = \mathcal{N}(\mathbf{z}_t; \alpha_t f_\varphi(\mathbf{x}, t), \sigma_t^2 I)$, which, unlike LSGM, transforms \mathbf{x} in a time-dependent manner. This forward process can also be described in terms of NFDM as $F_\varphi(\varepsilon, t, \mathbf{x}) = \alpha_t f_\varphi(\mathbf{x}, t) + \sigma_t\varepsilon$.

B.2. Connections of NFDM objective

In this section, we delve into the details of the NFDM’s objective function (eq. (18)), with a particular focus on the diffusion loss $\mathcal{L}_{\text{diff}}$ (eq. (20)).

First, let’s unpack the $\mathcal{L}_{\text{diff}}$ by substituting the definitions of \tilde{f}_φ^B and $\hat{f}_{\theta, \varphi}$:

$$\mathcal{L}_{\text{diff}} = \mathbb{E}_{u(t)q_\varphi(\mathbf{x}, \mathbf{z}_t)} \left[\frac{1}{2g_\varphi^2(t)} \left\| \tilde{f}_\varphi^B(\mathbf{z}_t, t, \mathbf{x}) - \hat{f}_{\theta, \varphi}(\mathbf{z}_t, t) \right\|_2^2 \right] \quad (43)$$

$$= \mathbb{E}_{u(t)q_\varphi(\mathbf{x}, \mathbf{z}_t)} \left[\frac{1}{2g_\varphi^2(t)} \left\| \underbrace{\left(f_\varphi(\mathbf{z}_t, t, \mathbf{x}) - f_\varphi(\mathbf{z}_t, t, \hat{\mathbf{x}}_\theta(\mathbf{z}_t, t)) \right)}_{\text{Flow Matching term}} + \frac{g_\varphi^2(t)}{2} \underbrace{\left(\nabla_{\mathbf{z}_t} \log q_\varphi(\mathbf{z}_t|\hat{\mathbf{x}}_\theta(\mathbf{z}_t, t)) - \nabla_{\mathbf{z}_t} \log q_\varphi(\mathbf{z}_t|\mathbf{x}) \right)}_{\text{Score Matching term}} \right\|_2^2 \right]. \quad (44)$$

This formulation clearly delineates two components of the objective: the first calculates the difference between the ODE drift terms, and the second calculates the difference between the score functions. Moreover, this expression highlights the role of $g_\varphi(t)$. When $g_\varphi(t)$ is small, the forward and reverse processes exhibit smoother trajectories, and the objective is dominated by the first term. Conversely, when $g_\varphi(t)$ is large, the processes exhibit more stochastic trajectories, and the objective is dominated by the second term.

Crucially, in the extreme scenarios where $g_\varphi(t)$ approaches either 0 or ∞ , the diffusion loss $\mathcal{L}_{\text{diff}}$ corresponds to either a reweighted Flow Matching loss (Lipman et al., 2022) or a reweighted Score Matching loss (Vincent, 2011), respectively:

$$\lim_{g_\varphi(t) \rightarrow 0} \mathcal{L}_{\text{diff}} = \lim_{g_\varphi(t) \rightarrow 0} \mathbb{E}_{u(t)q_\varphi(\mathbf{x}, \mathbf{z}_t)} \left[\frac{1}{2g_\varphi^2(t)} \left\| f_\varphi(\mathbf{z}_t, t, \mathbf{x}) - f_\varphi(\mathbf{z}_t, t, \hat{\mathbf{x}}_\theta(\mathbf{z}_t, t)) \right\|_2^2 \right], \quad (45)$$

$$\lim_{g_\varphi(t) \rightarrow \infty} \mathcal{L}_{\text{diff}} = \lim_{g_\varphi(t) \rightarrow \infty} \mathbb{E}_{u(t)q_\varphi(\mathbf{x}, \mathbf{z}_t)} \left[\frac{g_\varphi^2(t)}{4} \left\| \nabla_{\mathbf{z}_t} \log q_\varphi(\mathbf{z}_t|\hat{\mathbf{x}}_\theta(\mathbf{z}_t, t)) - \nabla_{\mathbf{z}_t} \log q_\varphi(\mathbf{z}_t|\mathbf{x}) \right\|_2^2 \right] \quad (46)$$

B.3. Connections of NFDM with Stochastic Interpolants

In this section, we explore the connections between NFDM and Stochastic Interpolants, as proposed by Albergo et al. (2023). Both NFDM and Stochastic Interpolants introduce a more general family of forward processes through the use of

a reparameterization function. Although we acknowledge the relevance of Stochastic Interpolants to our work, there are notable differences between the two approaches.

First, our methodology involves parameterizing the reverse process by substituting the prediction of \mathbf{x} into the forward process, whereas Stochastic Interpolants necessitate learning two separate functions for the reverse process: the velocity field and the score function.

Second, we present NFDM as a framework that enables both the pre-specification and learning of the forward process, in contrast to Stochastic Interpolants, which are derived under the assumption of a fixed forward process. Consequently, the objectives utilized by Stochastic Interpolants do not support the incorporation of learnable parameters for the forward process. Furthermore, these objectives are tailored towards learning the velocity field and the score function, rather than optimizing likelihood, as is the case with NFDM.

In their practical applications, Stochastic Interpolants are demonstrated with only simple parameterizations of the forward process. They propose a theoretical framework for learning the forward process that would result in an reverse process characterized by dynamical optimal transport. However, this approach is contingent upon solving a high-dimensional min-max optimization problem, for which they do not provide experimental results. Moreover, their work does not clearly articulate how Stochastic Interpolants might be applied to learning other generative dynamics.

In contrast, NFDM introduces a more generalized method for learning generative dynamics. Moreover, when NFDM is learned with restrictions or penalties (see Section 4), it remains within a min-min optimization paradigm, which can be addressed more efficiently.

C. Implementation details

Our evaluation of NFDM includes tests on synthetic data, CIFAR-10 (Krizhevsky et al., 2009), and two downsampled ImageNet (Deng et al., 2009; Van Den Oord et al., 2016) datasets. To maintain consistency with baselines, we employ horizontal flipping as a data augmentation technique in training models on CIFAR-10 and ImageNet (Song et al., 2020b; 2021). For density estimation of discrete data, uniform dequantization is used (see Appendix C.1).

We parameterize $\hat{\mathbf{x}}_\theta$ (eq. (17)) in the reverse process using a 5-layer perceptrons with 512 neurons in each layer for synthetic data and the U-Net architecture from Dhariwal & Nichol (2021) for images. In all experiments, a 3-layer perceptrons with 64 neurons in each layer is employed to parameterize g_φ (eq. (12)), and for F_φ (eq. (9)), we use an identical neural network to that of $\hat{\mathbf{x}}_\theta$. The sole difference is that for F_φ , we double the output of the last layer to parameterize $\bar{\mu}_\varphi$ (eq. (23)) and $\bar{\sigma}_\varphi$ (eq. (24)) with same model (see Section 3.5).

The models were trained using the Adam optimizer with the following parameters: $\beta_1 = 0.9$, $\beta_2 = 0.999$, a weight decay of 0.0, and $\epsilon = 10^{-8}$. The training process was facilitated by a polynomial decay learning rate schedule, which includes a warm-up phase for a predefined number of training steps. During this phase, the learning rate is linearly increased from 10^{-8} to a peak value. After reaching the peak learning rate, it is then linearly decreased to 10^{-8} by the final training step. The specific hyperparameters are detailed in Table 3. Training was carried out on Tesla V100 GPUs

C.1. Dequantization

For reporting the NLL, we employ standard uniform dequantization. The NLL is estimated using an importance-weighted average, given by

$$\log \frac{1}{K} \sum_{k=1}^K p_\theta(\mathbf{x} + u_k), \quad \text{where } u_k \sim \mathcal{U}(0, 1), \quad (47)$$

where $\mathbf{x} \in [0, \dots, 255]$.

C.2. Parameterization

We define the parameterization of the function F_φ as follows in eq. (22):

$$F_\varphi(\varepsilon, t, \mathbf{x}) = \mu_\varphi(\mathbf{x}, t) + \varepsilon \sigma_\varphi(\mathbf{x}, t). \quad (48)$$

Table 3. Training hyper-parameters.

	CIFAR-10	ImageNet 32	ImageNet 64
Channels	256	256	192
Depth	2	3	3
Channels multipliers	1,2,2,2	1,2,2,2	1,2,3,4
Heads	4	4	4
Heads Channels	64	64	64
Attention resolution	16	16,8	32,16,8
Dropout	0.0	0.0	0.0
Effective Batch size	256	1024	2048
GPUs	2	4	16
Epochs	1000	200	250
Iterations	391k	250k	157k
Learning Rate	4e-4	1e-4	1e-4
Learning Rate Scheduler	Polynomial	Polynomial	Constant
Warmup Steps	45k	20k	-

In addition to inferring F_φ , we require access to its inverse F_φ^{-1} and the logarithm of the determinant of the inverse transformation $\log |J_{F^{-1}}|$ (eq. (14)). The calculation of the inverse is straightforward:

$$F_\varphi^{-1}(\mathbf{z}_t, t, \mathbf{x}) = \frac{\mathbf{z}_t - \mu_\varphi(\mathbf{x}, t)}{\sigma_\varphi(\mathbf{x}, t)}. \tag{49}$$

The logarithm of the determinant of the inverse transformation, $\log |J_{F^{-1}}|$, can also be readily determined:

$$\log |J_{F^{-1}}| = -\log |J_F| = -\sum_{i=1}^D \log [\sigma_\varphi(\mathbf{x}, t)]_i, \tag{50}$$

where D represents the dimensionality of the data, and $[\sigma_\varphi(\mathbf{x}, t)]_i$ refers to i -th output of the σ_φ function.

To ensure the constraints $g_\varphi \geq 0$ (eq. (12)) and $\bar{\sigma}_\varphi \geq 0$ (eq. (24)) are met, we apply the softplus function to the outputs of the neural networks.